$N+\rho$ decay of baryons in a flux-tube-breaking mechanism

P. Stassart and Fl. Stancu
Institut de Physique B5, Université de Liège, Sart Tilman, B-4000 Liège 1, Belgium
(Received 15 December 1989)

A flux-tube-breaking mechanism motivated by QCD is extended to the analysis of the decay of nonstrange resonances into $N+\rho$. A proper threshold behavior is obtained by taking into account the instability of the ρ meson. The only parameter of the model has previously been fixed to adjust the decay of Δ into $N+\pi$. We find a good agreement with the few available data and make predictions for many other resonances where data are needed.

I. INTRODUCTION

The semirelativistic flux-tube constituent quark models[1,2] inspired by QCD are quite successful in predicting the spectra of hadrons.[3–5] Moreover, the flux-tube-breaking mechanism has been shown to provide a good description of the strong decay widths of mesons.[6,7] Its recent generalization[8] to the three-flux-tube picture of baryons met a similar success in describing the baryon decay into $N+\pi$.

A natural extension of our previous work is to study the nonstrange-baryon decay into $N+\rho$. It is possible that the flux-tube model describes the ρ meson better than the pion since the characteristics of the latter are more influenced by chiral-symmetry dynamics.[9] However, semirelativistic constituent quark models predict a correct ρ-π mass difference with interactions having parameters adjusted to fit the Δ-nucleon mass splitting.[3]

There are some theoretical studies[10,11] of the decay of resonances into $\Delta+\pi$ but, although similar in principle, the decay into $N+\rho$ in the frame of constituent quark models has been paid less attention. There is a study made by Koniuk,[12] where the escaping vector meson is treated as a point particle and the transition amplitude is obtained from the nonrelativistic reduction of the quark vector current. The restricted amount of theoretical work can be partly due to the absence of experimental evidence for a large number of resonances. Our results will be compared to those of Ref. 12 and to data, when available. We also show predictions for resonances where data are missing.

We briefly describe the flux-tube model in Sec. II. In order to calculate the $N+\rho$ correctly we have to treat ρ as an unstable particle. Its width allows for sizable subthreshold effects. The incorporation of the instability of ρ and its implication on the size of baryon resonance widths is presented in Sec. III. Section IV contains our results and a discussion.

II. THE FLUX-TUBE MODEL

The baryon and meson are treated as interacting qqq and $q\bar{q}$ systems, respectively. They are described by a QCD-inspired Hamiltonian[1] where the interaction potential is obtained by minimizing the energy of the gauge fields for fixed quark positions. In addition to the Coulomb-type and linear confinement terms the Hamiltonian also contains the hyperfine interaction[13] modified to include the finite size of the quark both in the spin-spin and tensor terms.

The baryon eigenstates used here come from the diagonalization[14,15] of the hyperfine interaction in the space of the $\mathbf{56}(0^+,2^+)$, $\mathbf{56}'(0^+)$, $\mathbf{70}(0^+,1^-,2^+)$, and $\mathbf{20}(1^+)$ SU(6) multiplets. The hyperfine interaction has two parameters, the quark mass m and its size Λ for which we take the so-called set II of Refs. 4 and 14:

$$m=324 \text{ MeV} \quad \text{and} \quad \Lambda=0.09 \text{ fm} . \tag{2.1}$$

The considered multiplets are built orthogonal to the variational ground state of Ref. 1 and contain up to two units of angular momentum and one unit of radial excitation. In Ref. 15 we showed that a radial shape, more consistent with the linear confinement than the conventional harmonic-oscillator shape,[1,14] lowers the position of the Roper resonance by about 100 MeV, bringing it to about 1500 MeV, i.e., much closer to the experimental value. In the following we shall use this type of radial excitation which influences the wave function of the P_{11} resonances. The rest is treated as in Ref. 14.

For the ρ meson we use the variational wave function provided by Ref. 3 where the mass difference π and ρ is obtained with the same parameters which also correctly reproduce quantities as, e.g., the nucleon-Δ mass splitting. Its radial part is

$$\Psi(r)=f^c(r)[1+u^\sigma(r)\boldsymbol{\sigma}_q\cdot\boldsymbol{\sigma}_{\bar{q}}] , \tag{2.2}$$

where $f^c(r)$—the central part—has been parametrized as

$$\begin{aligned} f^c(r)&=r^{-0.2}\exp\{-0.3965rW(r) \\ &\qquad -2.1r^{1.5}[1-W(r)]\} , \\ W(r)&=\frac{1+\exp(-0.15/0.05)}{1+\exp[(r-0.15)/0.05]} . \end{aligned} \tag{2.3}$$

In $W(r)$ the parameters are in fm. The spin-spin correlation function u^σ is defined by

$$u^{\sigma}(r)=\beta_{\sigma}\int \frac{e^{-\mu_{\sigma}|\mathbf{r}-\mathbf{r}'|}}{|\mathbf{r}-\mathbf{r}'|}V_{SS'}(r')d^3r' , \tag{2.4}$$

with

$$\beta_{\sigma}=2\ \text{GeV}^{-1}\,\text{fm}^{-2},\quad \mu_{\sigma}=4\ \text{fm}^{-1} \tag{2.5}$$

and

$$V_{ss}=\frac{1}{24\sqrt{\pi}m^2\Lambda^3}e^{-(r/2\Lambda)^2} , \tag{2.6}$$

in $\hbar=c=1$ units. As we proceed for the pion in Ref. 8 we parametrize the result of the integral (2.4) by an analytic expression in order to reduce the volume of the numerical computation involved by the calculation of the $N+\rho$ width (see next section). The parametric expression is

$$u^{\sigma}(r)=u^{\sigma}(0)\exp\{-\gamma_2 r^2 W(r)-\gamma_{15}r^{15}[1-W(r)]\}$$
$$W(r)=\frac{1+\exp(-r_0/a)}{1+\exp[(r-r_0)/a]} , \tag{2.7}$$

where by fitting the numerical values obtained for (2.4) we have

$$u^{\sigma}(0)=0.997\,43,\quad \gamma_2=8.11\ \text{fm}^{-2} ,$$
$$\gamma_{1.5}=3.9\ \text{fm}^{-1.5},\quad r_0=0.47\ \text{fm},\quad a=0.24\ \text{fm} .$$

The decay mechanism is the breaking of an infinite flux tube, commonly called the $^3P_0$ quark pair creation model.[16] It has been shown that this is a very good approximation to a finite extension QCD-inspired flux-tube breaking, both for meson[6] and baryon[8] decay.

The mechanism introduces only one parameter, γ_0, the breaking amplitude. Here it is kept at the value fixed to reproduce the $P_{33}(1232)\rightarrow N+\pi$ width,[8] so that no parameter has been varied in the following computations.

III. WIDTHS

The $R\rightarrow N+M$ partial transition amplitude is given by

$$\langle NM|T|R\rangle^{J_R}_{m_N m_M}=\sum_m \langle 11m\,-m\,|00\rangle\langle \phi_N^{m_N}\phi_M^{m_M}|\phi_R\phi_{\text{vac}}^{-m}\rangle I_m(R;N,M) , \tag{3.1}$$

where the notation is the same as in Ref. 8, with the addition of the J_R, m_N, and m_M indices, i.e., the total angular momentum of the resonance, the projections of the nucleon and meson spins, respectively. The matrix element $\langle \phi_N^{m_N}\phi_M^{m_M}|\phi_R\phi_{\text{vac}}^{-m}\rangle$ contains the spin-flavor part of the wave functions and $I_m(R;N,M)$ is a nine-dimensional integral[17] containing the overlap of the spatial part ψ of R, N, and M and the nonlocal meson emission operator

$$I_m(R;N,M)=-\left[\frac{3}{4\pi}\right]^{1/2}\frac{2^3}{(2\pi)^{3/2}}\delta(\mathbf{k}_M+\mathbf{k}_N)\gamma_0\int d^3\rho\, d^3\lambda\, d^3x\,\psi_R(\boldsymbol{\rho},\boldsymbol{\lambda}+(\tfrac{8}{3})^{1/2}\mathbf{x})\psi_N(\boldsymbol{\rho},\boldsymbol{\lambda})\exp\{i\mathbf{k}_M\cdot[(\tfrac{2}{3})^{1/2}\boldsymbol{\lambda}+\mathbf{x}]\}$$
$$\times\boldsymbol{\epsilon}_m\cdot(\mathbf{k}_M+i\nabla_x)\psi_M(2\mathbf{x}) , \tag{3.2}$$

where $\boldsymbol{\epsilon}_m$ is the spherical unit vector. This integral has been calculated with a Monte Carlo method. Since the rho is a spin-1 meson, two (for $J_R=\frac{1}{2}$ baryons) or three (for $J_R\geq\frac{3}{2}$ baryons) different $N+\rho$ partial waves can be observed. The corresponding amplitudes are then connected to the helicity amplitude (3.1) by the Jacob-Wick formula[18]

$$M^{J_R}_{ls}=\left[\frac{2l+1}{2J_R+1}\right]^{1/2}\sum_{m_N m_N}\langle 1s0m\,|J_R m\rangle\langle s_N s_M m_N-m_M|sm\rangle\langle NM|T|R\rangle^{J_R}_{m_N m_M} , \tag{3.3}$$

where l and s are the relative orbital momentum and total spin of the outgoing particles. s_N and s_M stand for the nucleon and the meson spin, respectively. For details about the helicity amplitudes, see Ref. 19.

In the rest frame of the resonance, a partial width is defined as

$$\Gamma_{ls}=\frac{1}{\pi}\frac{|M^{J_R}_{ls}|^2}{2J_R+1}\frac{kE_M E_N}{M_R}\langle I_N I_M I_{3N} I_{3M}|I_R I_{3R}\rangle^{-2} , \tag{3.4}$$

where k is the meson momentum, E_M its relativistic energy, E_N the relativistic recoil energy of the nucleon in its ground state, M_R the resonance mass, and the last factor a Clebsch-Gordan coefficient in the isospin space that reduces the calculation to $M=\rho^0$.

In contradistinction with the pion, the rho meson has a large width, so that the result obtained by inserting its nominal mass in Eqs. (3.1)–(3.4) can depart dramatically from the physical value, e.g., predicting a zero width for subthreshold resonances whereas sizable widths have been observed experimentally.

In order to provide appropriate threshold behavior we define Γ following a simplified version of the prescription given in Ref. 20 for "quasi-two-body" channels. Accordingly, we multiply (3.4) by a relativistic Breit-Wigner mass distribution σ and integrate over the mass of the rho resonance.[20] The width is then equal to

$$\Gamma_{ls}=\int_{(2m_{\pi})^2}^{(m_R-m_N)^2} dm_{\rho}^2\,\sigma(m_{\rho}^2)\Gamma_{ls}(m_{\rho}^2) , \tag{3.5}$$

where

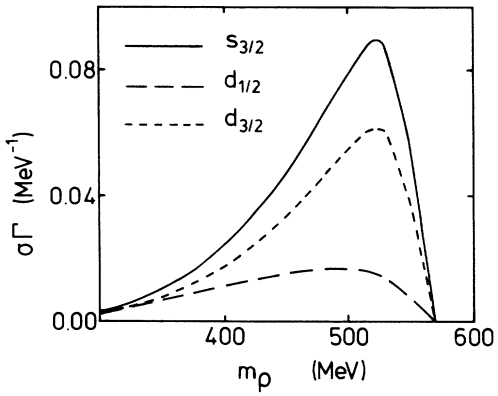

FIG. 1. The integrand $\sigma\Gamma_{ls}$ (MeV^{-1}) [Eq. (3.4)] as a function of m_ρ for the $D_{13}(1520)$ resonance, for its three partial waves.

$$\sigma(m_\rho^2)=\frac{\Gamma_\rho(m_\rho^2)m_\rho/\pi}{(M_\rho^2-m_\rho^2)^2+\Gamma_\rho^2(m_\rho^2)m_\rho^2} \tag{3.6}$$

and

$$\Gamma_\rho(m_\rho^2)=\Gamma_0\left[\frac{k}{k_0}\right]^3\frac{M_\rho}{m_\rho}\frac{2k_0^2}{k^2+k_0^2}$$

is the width of the ρ resonance.[21] Here $k(m_\rho^2)$ is the relative momentum of the pions in the decay $\rho\to\pi\pi$, M_ρ is the nominal rho mass, and $k_0=k(M_\rho^2)$. The nominal mass $M_\rho=770$ MeV and width $\Gamma_\rho(M_\rho^2)=153$ MeV are taken from the Particle Data Group.[22]

The lower integration limit in (3.5) corresponds to the $\rho\to\pi\pi$ threshold and the upper one to the $R\to N+\rho$ threshold.

A typical behavior of the integrand $\sigma(m_\rho^2)\Gamma(m_\rho^2)$ as a function of m_ρ is shown in Fig. 1 for a subthreshold resonance, namely, the $D_{13}(1520)$. Here we have three partial-wave contributions. They exhibit a typical pattern of subthreshold resonances: at small m_ρ, an increase governed by the form of σ up to a peak close to the $N+\rho$ threshold followed by a steep decrease down to zero, governed by the phase space.

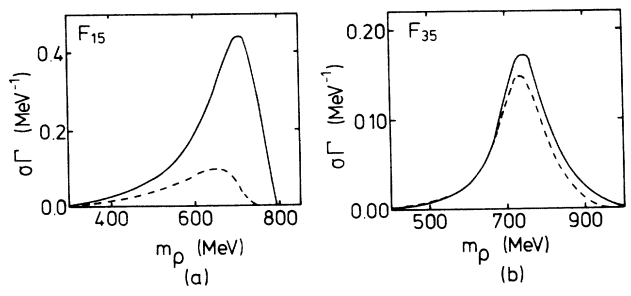

FIG. 2. $\sigma\sum_{l,s}\Gamma_{ls}$ (MeV^{-1}) as a function of m_ρ for (a) a close to threshold resonance, (b) a far above threshold resonance with the experimental (dashed) and the theoretical mass (solid).

IV. RESULTS AND DISCUSSION

In Table I, we present the square root $\Gamma_{N\rho}^{1/2}$ of the total $N\rho$ width

$$\Gamma_{N\rho}=\sum_{l,s}\Gamma_{ls} \tag{4.1}$$

for the 29 nonstrange resonances[14,15] described as excited quark states with up to two units of orbital excitation or one unit of radial excitation.

When the mass predicted by the model falls by more than 50 MeV off the experimental range, we have used the experimental mass[22] instead of the theoretical value. Indeed, if what we wish to test is not just the baryon spectra but rather the decay mechanism or the ρ wave function, we have to use a proper phase-space factor. This is not so important when the resonance is ≥ 200 MeV above the threshold, but it is essential when its mass lies close to threshold. We illustrate these considerations in Fig. 2 where we plot the product $\sigma\sum_{l,s}\Gamma_{ls}$ as a function of m_ρ. For the $F_{15}(1680)$ resonance [Fig. 2(a)], the theoretical mass is 1754 MeV, i.e., 44 MeV above threshold, while the experimental mass is 30 MeV below the threshold $M_N+M_\rho=1710$ MeV. Thus, the theoretical mass yields too large a phase-space factor and hence too large a width over the whole interval of (3.5). The experimental mass lowers the result of (3.5) by a factor of 4 and brings the width within experimental range. The theoretical model also overestimates the mass of the $F_{35}(1905)$ resonance by 57 MeV. However, as the threshold is much lower anyway, the plotted quantity [Fig. 2(b)] is not so sensitive to the replacement of the theoretical by the experimental mass. In this case the decrease of the total decay width is about 10% only.

The comparison of the calculated widths with the available experimental data[22] is made in Table I. The model predicts a value consistent with the experimental range for 10 out of the 13 resonances for which an interval or an upper limit exists. In particular, for the best known, i.e., the three four-star resonances, the theoretical values are all in agreement with experiment.

The largest discrepancies concern two one-star resonances $P_{11}(1440)$ and $S_{11}(1650)$, that need further experimental investigation. It should be noted that when the calculated width is less than 1 MeV, there is a large statistical Monte Carlo error. In particular, this is the case of the $S_{11}(1650)$ resonance.

It is also interesting and useful to compare the calculated partial-wave amplitudes with the experiment[22,23] for the three four-star resonances. This is done in Table II and one can see that the theoretical values and the experimentally available data are fairly close to each other. However, a phase disagreement appears for $S_{31}(1620)$.

Now we present some comments on the identification of the resonances in the context of $N+\rho$ decay. Our model[14] predicts two F_{35} resonances but only one has experimentally been seen in the $N+\pi$ decay. This well established resonance $F_{35}(1905)$ has been identified in our previous calculations[8,17] with the lowest member of the $J^\pi=\frac{5}{2}^+$ sector. It is located at 1962 MeV and its wave function is dominated by the $^2\Delta(70,2^+)$ multiplet. On

the other hand, a second resonance F_{35} has been seen in the $N+\rho$ decay. It is tempting to interpret it as the other member of the $J^{\pi}=\frac{5}{2}^{+}$ sector, having a mass of 1985 MeV and $\Gamma_{N\rho}^{1/2}=8.9$ MeV$^{1/2}$, satisfactorily consistent with an experimental mass of 2000–2200 MeV and a "large" $\Gamma_{N\rho}$ width.[22,24]

Another comment is related to the $\Delta\frac{1}{2}^{+}$ resonance. Our model predicts two such resonances of comparable mass 1910 and 1935 MeV, both consistent with the well established $P_{31}(1910)$ resonance. This makes its identification difficult and in fact the broad experimental range of masses (1850–1950) may offer room for two.[12,25] In the $N+\pi$ study[8,17] the observed $P_{31}(1910)$ resonance was interpreted as the first in the sector. But the $N+\rho$ decay widths would be more in agreement with data if we interpret it as the second in the sector, i.e., having a mass of 1935 MeV and as main component the $^{4}\Delta(56,2^{+})\frac{1}{2}^{+}$, as in Ref. 25. The calculation would then give $\Gamma_{N\rho}\cong 49$ MeV, i.e., "small", as indicated by the data. For the other we get $\Gamma_{N\rho}=294$ Mev, which is too large. In this reinterpretation of the $P_{31}(1910)$ the agreement with $\Gamma_{N\pi}$ would not be altered as indicated in Table III. Moreover, the photodecay amplitude becomes more consistent with experiment. It is possible that the very large $N+\rho$ width, if confirmed, is the cause for not observing a $^{2}\Delta(70,0^{+})\frac{1}{2}^{+}$ main component resonance in the partial-

TABLE I. Square root of the decay widths $\Gamma_{N\rho}^{1/2}$ (MeV$^{1/2}$). First column: resonance, partial-wave notation $L_{2I\,2J}$ (the experimental mass is indicated when an identification has been proposed). Second column: main component (Refs. 14 and 15). Third column: theoretical mass (Refs. 14 and 15). Fourth column: theoretical value, index e indicates that the experimental mass has been used in calculating the width (see text for discussion). Fifth column: Ref. 12. Sixth column: experimental value when available (Ref. 22). Seventh column: status as seen in $N\rho$ decay (Ref. 22).

Resonance	Main component	Mass	This work	Ref. 12	Expt.	Status
$F_{17}(1990)$	$^{4}N(70,2^{+})\frac{7}{2}^{+}$	1980	1.1	4.3		
$F_{37}(1950)$	$^{4}\Delta(56,2^{+})\frac{7}{2}^{+}$	1952	4.5	9.5	<5.8	*
$F_{15}(1680)$	$^{2}N(56,2^{+})\frac{5}{2}^{+}$	1754	4.3^{e}	4.5	4.3 ± 1.0	****
$F_{15}(2000)$	$^{2}N(70,2^{+})\frac{5}{2}^{+}$	1970	4.2	8.2		
F_{15}	$^{4}N(70,2^{+})\frac{5}{2}^{+}$	2033	4.3	8.1		
$F_{35}(1905)$	$^{2}\Delta(70,2^{+})\frac{5}{2}^{+}$	1962	5.1^{e}	6.7	<12.2	*
$F_{35}(2000)$	$^{4}\Delta(56,2^{+})\frac{5}{2}^{+}$	1985	8.9	19.7	Large	**
$P_{13}(1720)$	$^{2}N(56,2^{+})\frac{3}{2}^{+}$	1752	5.2	12.5	<13.7	*
P_{13}	$^{4}N(70,0^{+})\frac{3}{2}^{+}$	1914	6.1	1.5		
P_{13}	$^{4}N(70,0^{+})\frac{3}{2}^{+}$	1979	5.7	8.1		
P_{13}	$^{2}N(20,1^{+})\frac{3}{2}^{+}$	1985	3.3	8.4		
P_{13}	$^{2}N(20,1^{+})\frac{3}{2}^{+}$	2046	2.8	3.9		
$P_{33}(1232)$	$^{4}\Delta(56,0^{+})\frac{3}{2}^{+}$	1285	0.0			
$P_{33}(1600)$	$^{4}\Delta(56',0^{+})\frac{3}{2}^{+}$	1904	2.9	5.7		*
$P_{33}(1920)$	$^{4}\Delta(56,2^{+})\frac{3}{2}^{+}$	1964	5.2	11.6		
P_{33}	$^{2}\Delta(70,2^{+})\frac{3}{2}^{+}$	1979	9.1	5.9		
$P_{11}(1440)$	$^{2}N(56',0^{+})\frac{1}{2}^{+}$	1485	1.5	0.3	$5.0^{+2.2}_{-1.5}$	*
$P_{11}(1710)$	$^{2}N(70,0^{+})\frac{1}{2}^{+}$	1796	4.1^{e}	6.0	$4.7^{+2.1}_{-2.6}$	*
P_{11}	$^{4}N(70,2^{+})\frac{1}{2}^{+}$	1930	1.9	4.7		
P_{11}	$^{2}N(20,1^{+})\frac{1}{2}^{+}$	2042	0.3	1.3		
P_{31}	$^{2}\Delta(70,0^{+})\frac{1}{2}^{+}$	1910	17.1	7.9		
$P_{31}(1910)$	$^{4}\Delta(56,2^{+})\frac{1}{2}^{+}$	1935	6.9	6.1	Small	*
$D_{15}(1675)$	$^{4}N(70,1^{-})\frac{5}{2}^{-}$	1653	2.0	2.3	<4.2	*
$D_{13}(1520)$	$^{2}N(70,1^{-})\frac{3}{2}^{-}$	1496	4.6	5.2	$5.0^{+0.9}_{-1.1}$	****
$D_{13}(1700)$	$^{4}N(70,1^{-})\frac{3}{2}^{-}$	1714	3.7	5.1	<4.9	*
$D_{33}(1700)$	$^{2}\Delta(70,1^{-})\frac{3}{2}^{-}$	1631	4.9^{e}	17.0	<10.2	**
$S_{11}(1535)$	$^{2}N(70,1^{-})\frac{1}{2}^{-}$	1475	1.1^{e}	6.3	~2.7	**
$S_{11}(1650)$	$^{4}N(70,1^{-})\frac{1}{2}^{-}$	1627	0.6	10.1	$5.1^{+2.7}_{-2.9}$	*
$S_{31}(1620)$	$^{2}N(70,1^{-})\frac{1}{2}^{-}$	1631	4.4	8.0	$4.6^{+1.1}_{-1.1}$	****

TABLE II. $N\rho$ decay amplitudes ($\mathrm{MeV}^{1/2}$) of four-star resonances. First row is our calculation, second is Ref. 12, and third is the experimental value (Refs. 22 and 23), when available. The phase convention is that of Ref. 12.

Resonance	$s_{\frac{1}{2}}$	$s_{\frac{3}{2}}$	$p_{\frac{3}{2}}$	$d_{\frac{1}{2}}$	$d_{\frac{3}{2}}$	$f_{\frac{1}{2}}$	$f_{\frac{3}{2}}$
			+4.0			−1.6	+1.3
$F_{15}(1680)$			+3.1			−1.3	+2.7
			$+3.8^{+0.6}_{-0.8}$				+2.2±0.7
		+5.0		−0.7	+1.1		
$D_{13}(1520)$		+3.2		−1.7	−2.7		
		$+4.4^{+1.1}_{-1.2}$					
	−7.8				+1.7		
$S_{31}(1620)$	+2.5				−3.6		
	$-3.9^{+2.6}_{-2.3}$				+2.8±0.9		

wave analysis.

As described in Sec. III the same transition operator has been used both in the $N+\pi$ and $N+\rho$ decays. It is therefore useful to collate the results of the present work with those obtained previously[8] for the $N+\pi$ decay. The $N+\pi$ study concerned 19 resonances rated as two-, three-, or four-star. An appropriate pion wave function lead globally to a satisfactory agreement. Some noticeable departures from data still remained. Among them we should be especially concerned with the $P_{13}(1720)$ and $S_{31}(1620)$ that we included in the comparison with the $N\rho$ data. Their calculated $N\pi$ width is a factor of 4 off the average experimental width. In this situation we may question, of course, the state composition of these resonances. The resonance $S_{31}(1620)$ that belong to the negative-parity spectrum has been treated as an isolated state in the diagonalization[14] of the hyperfine interaction. The addition of the $N=3$ shell[19] should be considered to see whether the situation can be improved for this particular case.

It is natural to compare our results with those of Koniuk.[12] The partial-wave amplitudes for the three four-star resonances under study are compared in Table II. Aside from the $S_{31}(1620)$ resonance discussed above there are no large differences between the two sets of results. The total widths, that we compare in Table I for all resonances considered in the calculation, have a similar order of magnitude in most cases. The largest differences which appear are not relevant for the quality of the models inasmuch as they usually refer to one- or two-star resonances.

Although the two approaches seem to have similar performances we have to bear in mind that in Ref. 12 there are two free parameters and in our calculations there is none. Hence the breaking mechanism of an infinite flux tube has more predictive power. The effective coupling of Ref. 12 may mock up some nonlocality effects[11] which in our work appear through the finite size of the emitted meson.[8] But at the level of pure numerical comparison it would be difficult to have a deeper understanding of those parameters.

In conclusion, we have calculated $N+\rho$ decay widths based on a generalization of the flux-tube-breaking mechanism to three flux tubes. The same formalism has been applied to $N+\pi$ decay in a previous study. The present extension was natural because ρ and π are treated as $q\bar{q}$ pairs with a correct mass splitting obtained from a color-magnetic interaction which also reproduces the N-Δ splitting. There is no free parameter in the $N+\rho$ calculations and we obtain good agreement with the experimental widths listed by the Particle Data Group.[22] The agreement between theory and data can serve as an additional help to the identification of some resonances. We also provide predictions for many resonances for which an $N+\rho$ decay exists in principle. New experimental measurements of $N+\rho$ decay are highly desirable for resonances located in the range 1.5–2.5 GeV. They could provide additional help in testing the state composition of the calculated resonances.

TABLE III. Photodecay amplitudes and square root of $N\pi$ and $N\rho$ decay widths ($\mathrm{MeV}^{1/2}$) of $\Delta_{\frac{1}{2}}{}^{+}$. First row: $^2\Delta(70,0^+)$ main component state. Second row: $^4\Delta(56,2^+)$ main component state. Third row: experiment (Ref. 22).

	Mass	$A^{\rho}_{1/2}$	$\Gamma^{1/2}_{N\pi}$	$\Gamma^{1/2}_{N\rho}$
$^2\Delta(70,0^+)_{\frac{1}{2}}{}^{+}$	1910	+31	5.4	17.1
$^4\Delta(56,2^+)_{\frac{1}{2}}{}^{+}$	1935	−6	6.8	6.9
Experiment	1910	−12±30	$6.6^{+1.1}_{-1.3}$	Small

ACKNOWLEDGMENTS

One of us (F.S.) would like to thank Byron Jennings for an inspiring discussion. We are grateful to J. Kogut and S. Kumano for kindly providing the variational parameters of the ρ-meson function. One of us (P.S.) acknowledges support from the Institut Interuniversitaire des Sciences Nucléaires, Belgium.

[1]J. Carlson, J. Kogut, and V. R. Pandharipande, Phys. Rev. D **27**, 23 (1983).
[2]N. Isgur and J. Paton, Phys. Rev. D **31**, 2910 (1985).
[3]J. Carlson, J. Kogut, and V. R. Pandharipande, Phys. Rev. D **28**, 2808 (1983).
[4]R. Sartor and Fl. Stancu, Phys. Rev. D **31**, 128 (1985).
[5]C. Capstick and N. Isgur, Phys. Rev. D **34**, 2809 (1986).
[6]R. Kokoski and N. Isgur, Phys. Rev. D **35**, 907 (1987).
[7]S. Kumano and V. R. Pandharipande, Phys. Rev. D **38**, 146 (1988).
[8]Fl. Stancu and P. Stassart, Phys. Rev. D **39**, 343 (1989).
[9]See, e.g., W. Weise, in *Nuclear Structure at High Spin, Excitation, and Momentum Transfer,* Bloomington, Indiana, 1985, edited by Hermann Nann (AIP Conf. Proc. No. 142) (AIP, New York, 1986), p. 403.
[10]R. Koniuk and N. Isgur, Phys. Lett. **44**, 845 (1980).
[11]M. B. Gavela, A. Le Yaouanc, L. Oliver, O. Pène, J.-C. Raynal, and S. Sood, Phys. Rev. D **21**, 182 (1980).
[12]R. Koniuk, Nucl. Phys. **B195**, 452 (1982).
[13]A. de Rújula, H. Georgi, and S. L. Glashow, Phys. Rev. D **12**, 147 (1975).
[14]R. Sartor and Fl. Stancu, Phys. Rev. D **34**, 3405 (1986).
[15]Fl. Stancu and P. Stassart, Phys. Rev. D **41**, 916 (1990).
[16]A. Le Yaouanc, L. Oliver, O. Pène, and J.-C. Raynal, Phys. Rev. D **8**, 2223 (1973).
[17]Fl. Stancu and P. Stassar, Phys. Rev. D **38**, 233 (1988).
[18]M. Jacob and G. C. Wick, Ann. Phys. (N.Y.) **7**, 404 (1959).
[19]P. Stassart, Ph.D. thesis, University of Liège, 1990.
[20]R. E. Cutkosky, C. P. Forsyth, R. E. Hendrick, and R. L. Kelly, Phys. Rev. D **20**, 2839 (1979).
[21]J. D. Jackson, Nuovo Cimento **34**, 6 (1964).
[22]Particle Data Group, G. P. Yost *et al.*, Phys. Lett. B **204**, 1 (1988).
[23]R. S. Longacre *et al.*, Phys. Lett. **55B**, 415 (1975); Phys. Rev. D **17**, 1795 (1978); R. S. Longacre *et al.*, Nucl. Phys. **B108**, 365 (1976); R. S. Longacre and J. Dolbeau, *ibid.* **B122**, 493 (1977).
[24]D. M. Manley *et al.*, Phys. Rev. D **30**, 904 (1984); D. M. Manley, Phys. Rev. Lett. **52**, 2122 (1984).
[25]N. Isgur and G. Karl, Phys. Rev. D **19**, 2653 (1979).